Phytopathology Research

RESEARCH

Open Access

# The bZIP transcription factor UvbZIP6 mediates fungal growth, stress response, and false smut formation in *Ustilaginoidea virens*

Jinsong Qu†, Yufu Wang†, Minzheng Cai, Yueran Liu, Lifan Gu, Peng Zhou, Yulin Du, Chenghui Xu, Rui Wang, Weixiao Yin* and Chaoxi Luo

## Abstract

Rice false smut, caused by *Ustilaginoidea virens*, is one of the most destructive diseases in major world rice-producing regions. Basic leucine zipper (bZIP) proteins, which belong to an evolutionarily conserved transcription factor family and play critical roles in various biological processes in eukaryotes, have been previously identified in *U. virens*; however, their functions still need to be further elucidated. Therefore, we aimed to analyze the biological roles of UvbZIP6, a member of the bZIP family in *U. virens*. In this study, we found that *UvbZIP6* was highly up-regulated at 7 days post-inoculation. Deletion of *UvbZIP6* in *U. virens* resulted in an increase in fungal growth and sensitivity to Congo red and calcofluor white, whereas a decrease in sensitivity to hyperosmotic, oxidative, and sodium dodecyl sulfate stresses. Conidiation capacity was reduced in *UvbZIP6*-knockout mutants, but conidial morphology and germination were not affected. Although *UvbZIP6*-knockout mutants caused infection in rice plants, they could not form false smut balls. Our study indicates that UvbZIP6 is required for fungal growth, conidiation, stress response, and false smut ball formation of *U. virens*.

**Keywords:** Rice false smut, *Ustilaginoidea virens*, bZIP proteins, UvbZIP6, False smut formation

## Background

Transcription factors (TFs) are proteins that bind to specific DNA sequences of their target genes to regulate gene transcription and thus play an essential role in modulating growth, development, and stress tolerance (Lambert et al. 2018). Basic leucine zipper (bZIP) proteins form a superfamily of TFs and are found across eukaryotes. The bZIP proteins are involved in various biological processes, such as resistance to abiotic and biotic stresses, seed germination and development, morphogenesis, and hormonal regulation (Zhang et al. 2016; Dröge-Laser et al. 2018; Dröge-Laser and Weiste 2018; Hao et al. 2019).

In plants, bZIP proteins play a variety of functions, including the development of seeds and flowers, hormone synthesis and signal transduction, and response to abiotic and biotic stresses. Overexpression of *ZmbZIP4* in maize promotes root development and enhances abscisic acid synthesis, resulting in increased plant tolerance to abiotic stresses (Ma et al. 2018). The apple bZIP protein MdHY5 regulates the transcription of *MdMYB10* and anthocyanin biosynthesis genes, promoting the expression of nitrate reductase genes and nitrate uptake genes and thereby playing essential roles in anthocyanin accumulation and nitrate assimilation (An et al. 2017). The bZIP protein OsABF1 contributes to drought tolerance in rice by regulating the expression of *COR413-TM1*, which encodes a putative

†Jinsong Qu and Yufu Wang contributed equally to this work.

*Correspondence: wxyin@mail.hzau.edu.cn

Hubei Key Laboratory of Plant Pathology, College of Plant Science and Technology, Huazhong Agricultural University, Wuhan 430070, China

thylakoid membrane protein. Moreover, OsABF1 directly regulates the expression of various genes, forming a complex feedback circuit in the drought or abscisic acid signaling pathway (Zhang et al. 2017). In *Japonica* rice, bZIP73 (bZIP73$^{Jap}$) interacts with bZIP71 to modulate abscisic acid and reactive oxygen species (ROS) homeostasis, thus enhancing rice adaptation to cold climates (Liu et al. 2018). The endoplasmic reticulum (ER) membrane-associated TF OsbZIP74 in rice plays an essential role in unfolding proteins induced by heat stress (Lu et al. 2012). The plasma membrane-associated NAC transcription factor OsNTL3 regulates the expression of *OsbZIP74* by binding to its promoter under heat stress, and in turn, OsbZIP74 also regulates the expression of *OsNTL3*. Therefore, OsbZIP74 and OsNTL3 can form a circuit to adapt to heat stress by regulating the interactions between the ER, plasma membrane, and nucleus (Liu et al. 2020).

Numerous bZIP proteins have been identified in filamentous fungi and oomycetes, a few of which are involved in the development, nutrient utilization, and stress responses. Overexpression of *RsmA*, a bZIP TF-coding gene in *Aspergillus nidulans*, significantly increases secondary metabolite production and confers resistance against predation. Furthermore, RsmA binds to the promoter region of *aflR* in the sterigmatocystin gene cluster, which encodes a C6 TF (Yin et al. 2012). MetR regulates sulfur assimilation and affects iron balance, and it therefore essential for the pathogenicity of *Aspergillus fumigatus* (a human pathogen) (Amich et al. 2013). Under $H_2O_2$ stress conditions, fission yeast increases the expression levels of bZIP TF genes *ATF1* and *PCR1* to successfully adapt to oxidative stress (Fernández-Vázquez et al. 2013). The bZIP protein HapX in *Fusarium oxysporum* plays a primary role in iron homeostasis, virulence, and rhizosphere competence (López-Berges et al. 2012). In *Fusarium graminearum*, Fpo1, a negative regulator of perithecium development, is crucial for vegetative growth, asexual sporulation, and virulence. Deletion of *Fpo1* results in reprogramming of the carbon metabolism, including fatty acid production, which is essential for sexual reproduction (Shin et al. 2020). Mrap1 regulates fungal morphology, virulence, and microsclerotia formation in *Metarhizium rileyi* (Song et al. 2018). VdAtf1 is necessary for penetration peg formation and contributes to pathogenicity by regulating nitric oxide (NO) resistance and inorganic nitrogen metabolism in *Verticillium dahliae* (Tang et al. 2020). Systematic characterization of the bZIPs in *Magnaporthe oryzae* reveals the regulatory mechanisms underlying fungal growth, conidiation, environmental stresses, host penetration, and pathogenicity (Kong et al. 2015; Tang et al. 2015).

*Ustilaginoidea virens* is the causal agent of rice false smut, one of the most destructive rice diseases in rice-producing areas worldwide. The typical symptom is the development of yellowish-orange or dark-green smut balls. In addition to the yield loss, ustiloxins produced by *U. virens* are harmful to humans and animals (Hu et al. 2019). With the release of genome data and the development of an efficient CRISPR-Cas9 system to knock out genes, research on gene functions, including TF-coding genes, has been accelerated in *U. virens* (Zhang et al. 2014; Liang et al. 2018). The conserved fungal-specific TF UvPRO1 is essential for hyphal growth, conidiation, stress tolerance, and pathogenesis (Lv et al. 2016). The homeobox transcription factor UvHOX2 contributes to chlamydospore formation, conidiation, and pathogenicity (Yu et al. 2019).

Previously, we have identified the bZIP genes in *U. virens* (Yin et al. 2017), but their functions are still unknown. In this study, the biological roles of UvbZIP6 were evaluated by knocking out the gene in *U. virens*. The results indicate that UvbZIP6 is involved in fungal growth, conidiation, and stress responses of *U. virens*. Additionally, we found that *UvbZIP6*-knockout mutants could establish successful infection in rice plants but could not generate false smut balls, indicating that UvbZIP6 contributes to false smut formation.

## Results

### Sequence analysis of UvbZIP6

To investigate the function of bZIP proteins in *U. virens*, we selected a putative UvbZIP6 protein (GenBank: KDB14749.1) of 254 amino acids (aa) as a reference for further research. We amplified the corresponding sequence of *UvbZIP6* from the *U. virens* strain JS60-2. The results showed that it encodes a 265-aa protein (Additional file 1: Figure S1). In addition, UvbZIP6 contains a bZIP domain, and the amino acid at position 17 is glutamic instead of glutamine. The orthologs of UvbZIP6 were also found in *Pochonia chlamydosporia* and three *Metarhizium* species; sequence alignment analysis showed that they are conserved in these species, especially for the bZIP domain (Fig. 1a). Phylogenetic analysis was performed with UvAP1 (GenBank: KDB19098.1) as the outgroup, which is an ortholog of the *M. oryzae* bZIP TF MoAP1 and shares low similarity with UvbZIP6. The result further indicated the conservation of UvbZIP6 in these five fungal species (Fig. 1b). Moreover, the orthologs of UvbZIP6 are not widely distributed in fungi, indicating their potential unique role in a few species.

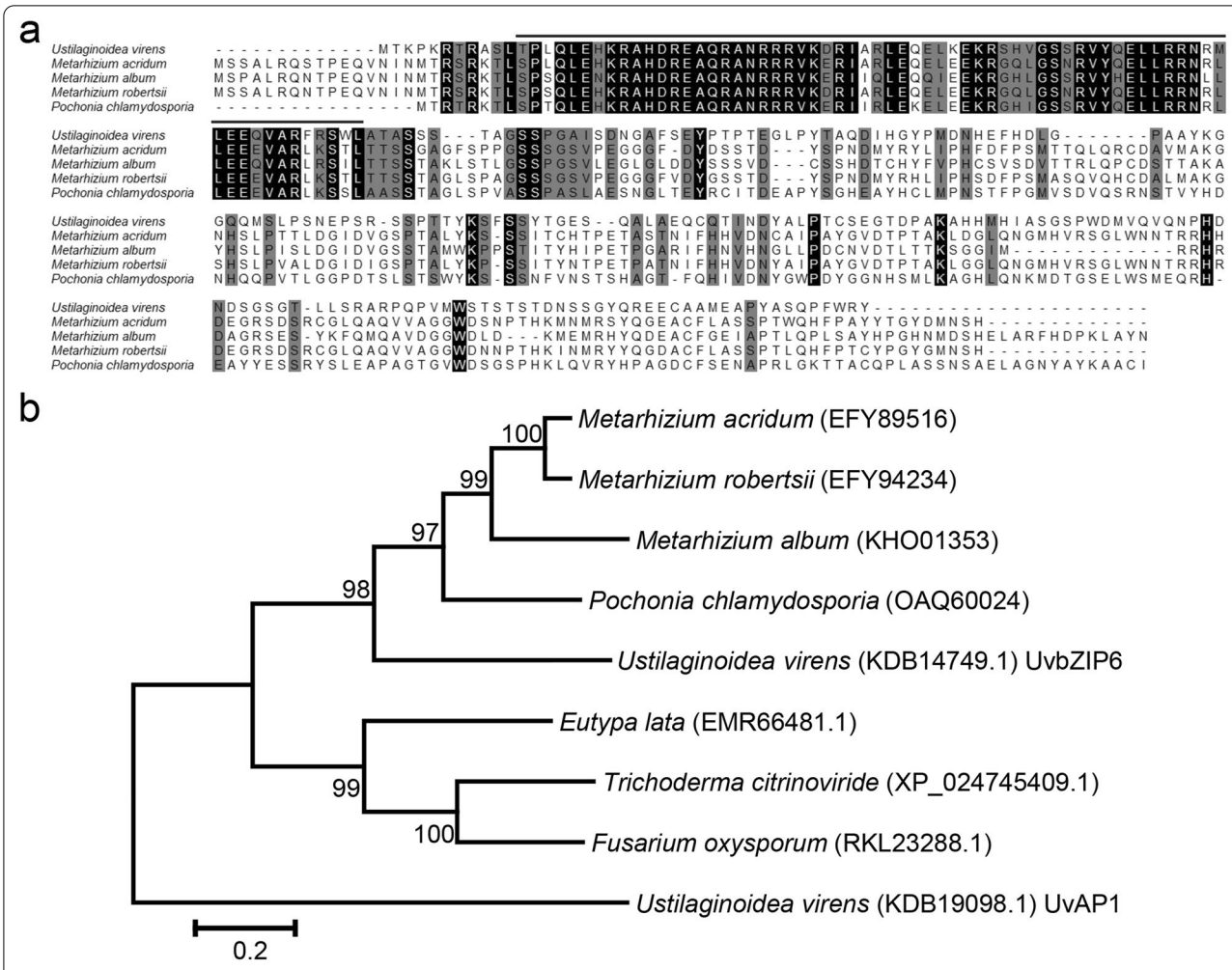


**Fig. 1** Alignment and phylogenetic analysis of UvbZIP6. **a** Sequence alignment of UvbZIP6 and its orthologs from five different fungal species. The bZIP domain sequence indicated by the line was predicted using the SMART website. **b** Phylogenetic analysis of UvbZIP6. The phylogenetic tree was constructed using MEGA7, and UvAP1 (KDB19098) was used as the outgroup

### Expression profile of *UvbZIP6* at different stages of *U. virens* infection

To gain insights into the possible function of *UvbZIP6*, we performed quantitative real-time PCR (qPCR) analysis to evaluate its expression at different infection stages. The results showed that the expression level of *UvbZIP6* gradually increased after inoculation and peaked at 7 days post-inoculation (dpi) (Fig. 2), coinciding with the time point when *U. virens* shows a successful infection, which is reflected by the generation of abundant mycelia in rice spikelets (Song et al. 2016). This suggests that UvbZIP6 may play a crucial role during the stage of *U. virens* infection.

### *UvbZIP6* gene deletion and Δ*UvbZIP6* mutant complementation

To characterize the biological function of *UvbZIP6*, we knocked out the gene using the method previously described (Xie et al. 2019). The fragments flanking approximately 1.5 kb upstream or downstream of the *UvbZIP6* ORF region were fused with the part of the hygromycin B phosphotransferase gene (*hph*). The pCAS9:tRp-gRNA vector was constructed as described previously (Liang et al. 2018). We generated the *UvbZIP6* deletion mutants by replacing the ORF of *UvbZIP6* in the wild-type (WT) strain JS60-2 with the donor template containing *hph* via the transformation of protoplasts with

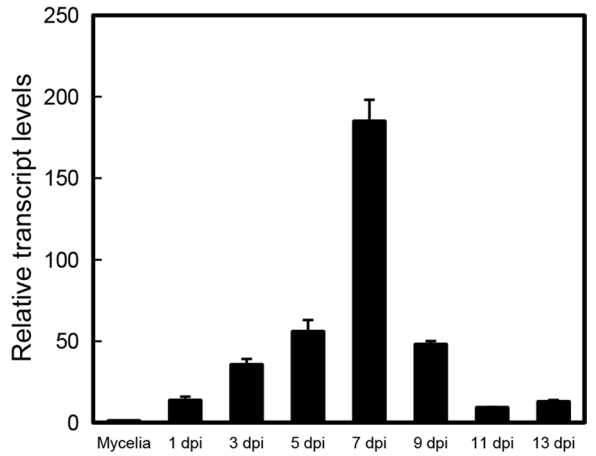


**Fig. 2** Transcriptional expression of *UvbZIP6* at different stages of *U. virens* infection. The expression of *UvbZIP6* was investigated by qPCR. The *β-tubulin* gene was used as an internal reference, and the mycelial expression level was normalized to 1.0. The experiment was repeated three times independently. Three replicates were considered for each independent test, and the error bar represents the standard deviation

linear donor DNA fragments and the pCAS9:tRp-gRNA vector. The transformants were verified by PCR amplification using different primer pairs (Additional file 1: Figure S2a, b and Additional file 2: Table S1). Furthermore, the complemented strains were obtained by introducing the ORF sequence of *UvbZIP6* containing the native promoter region, into the Δ*UvbZIP6*-5 mutant (Additional file 1: Figure S3a, b). The expression of *UvbZIP6* in the Δ*UvbZIP6* mutants and complemented strains was detected by reverse transcription PCR (RT-PCR) (Additional file 1: Figure S4). These results showed that *UvbZIP6* was completely inactivated in the Δ*UvbZIP6* mutants, while its transcript levels in the WT and complemented strains were similar.

### UvbZIP6 is involved in vegetative growth and conidiation in *U. virens*

To investigate the role of UvbZIP6 in mycelial growth, we incubated the WT strain, Δ*UvbZIP6* mutants, and complemented strains on three different media (PSA, YTD, and PDA). Compared with the WT and complemented strains, the Δ*UvbZIP6* mutants showed a higher growth rate on PSA and PDA media; however, the growth rate did not differ significantly among these three strains on YTD medium (Fig. 3a, b). In addition, the mycelial dry weights were measured, and the Δ*UvbZIP6* mutants showed higher biomass than the WT and complemented

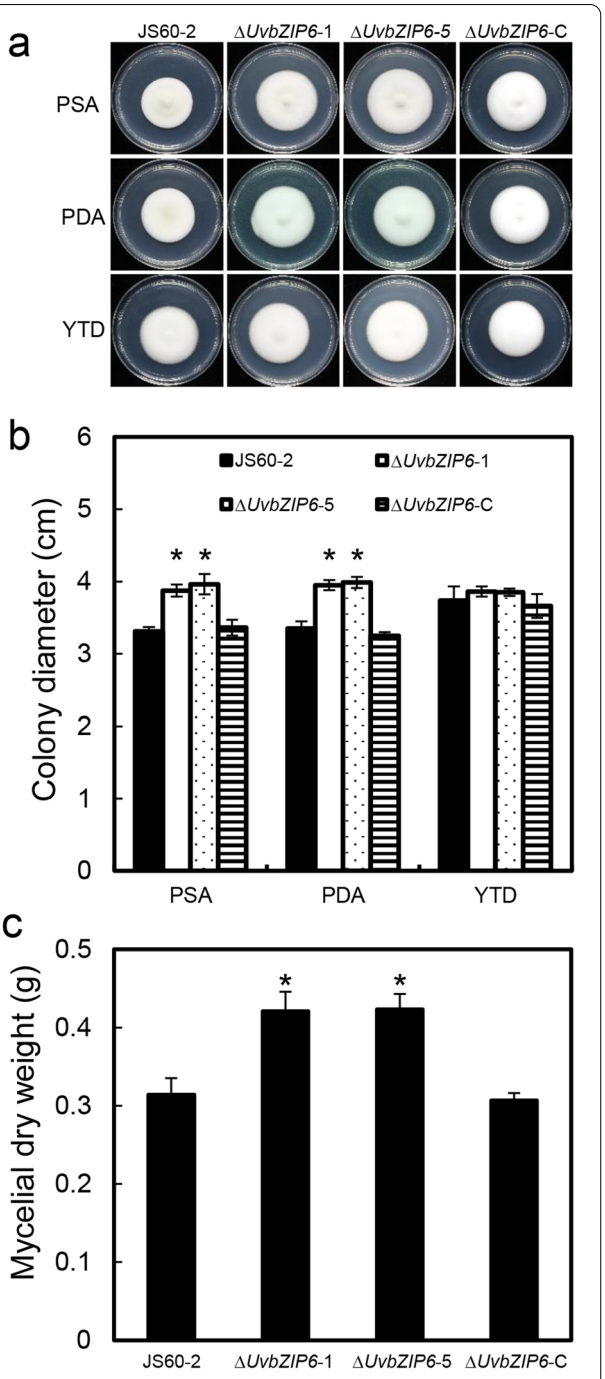


**Fig. 3** Knockout of *UvbZIP6* enhances the vegetative growth of *U. virens*. **a** Colony morphology of *U. virens* strains on PSA, PDA, and YTD. The WT, *UvbZIP6*-knockout mutants, and complemented strains were incubated on the medium at 27 °C for 14 days. **b** Colony diameter of *U. virens* strains on different media. **c** Mycelia dry weight of the tested strains. The mycelia were collected and dried after incubation in PSB at 27 °C for 7 days. The error bars represent the standard deviation, and asterisks represent a significant difference ($P < 0.05$)

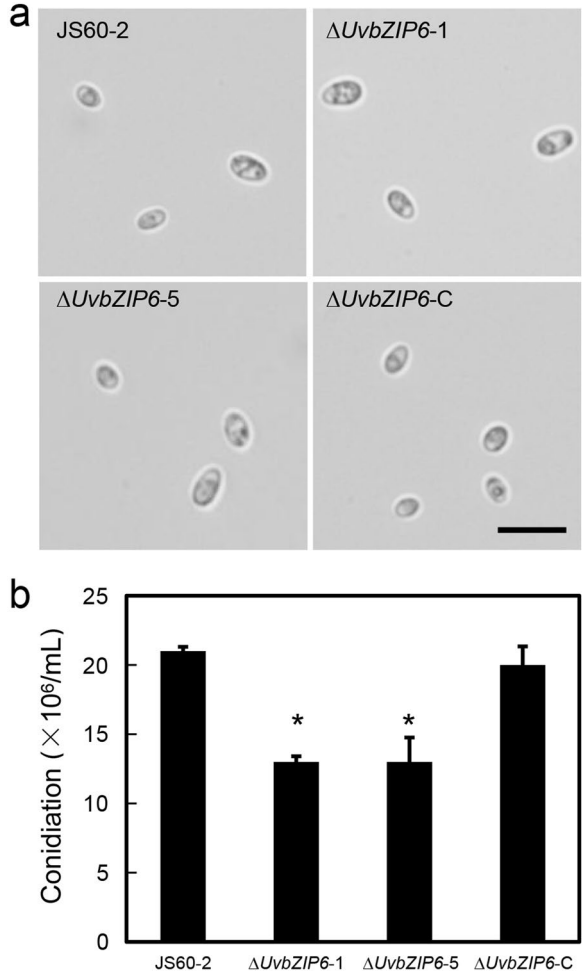


**Fig. 4** Knockout of *UvbZIP6* reduces conidiation in *U. virens*. **a** Conidial morphology of the WT, *UvbZIP6*-knockout mutants, and complemented strains. The strains were cultured in PSB at 27 °C for 7 days. Scale bar = 10 μm. **b** Conidiation capacity of the tested strains. Error bars represent standard deviation, and asterisks denote a significant difference ($P < 0.05$)

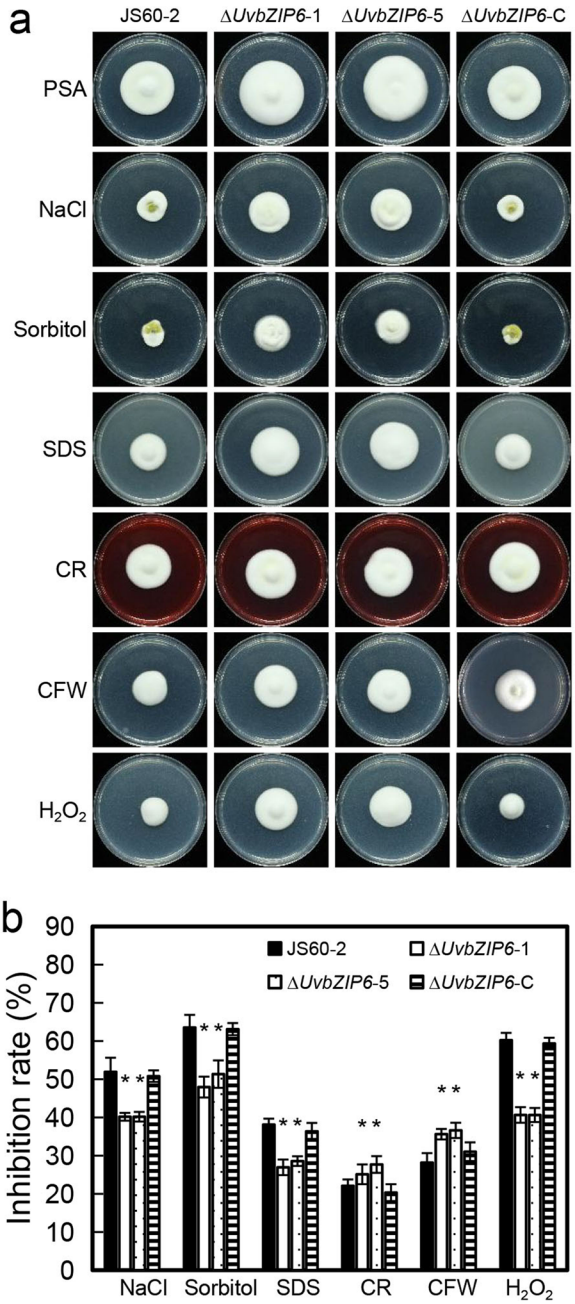


**Fig. 5** UvbZIP6 regulates stress responses of *U. virens*. **a** Colony morphology of *U. virens* strains on media with different stress agents. The strains were cultured on PSA plates with 0.5 M NaCl, 0.9 M sorbitol, 0.04% sodium dodecyl sulfate (SDS), 200 μg/mL Congo red (CR), 120 μg/mL calcofluor white (CFW), or 0.03% $H_2O_2$ for 14 days. **b** Inhibition rates of different stress agents on vegetative growth of the tested *U. virens* strains. The asterisks represent a significant difference ($P < 0.05$)

strains (Fig. 3c). These results suggest that UvbZIP6 is a negative regulator of vegetative growth.

The conidial production was also examined to investigate whether UvbZIP6 is involved in conidiation. The results showed that conidiation was significantly reduced in the Δ*UvbZIP6* mutants compared with that in WT and complemented strains (Fig. 4). However, no difference was observed in conidial morphology and germination among WT, Δ*UvbZIP6*, and complemented strains (Fig. 4a and Additional file 1: Figure S5). These results indicate that UvbZIP6 contributes to the conidiation in *U. virens*.

#### UvbZIP6 is involved in stress responses of *U. virens*

To explore whether UvbZIP6 is involved in stress response, the strains were cultured on PSA medium supplemented with different stress-inducing agents. Compared with the WT and complemented strains, Δ*UvbZIP6* mutants showed a lower growth inhibition

rate under hyperosmotic and oxidative stresses (Fig. 5). In contrast, a higher inhibition rate was observed on plates with Congo red (CR) or calcofluor white (CFW) (Fig. 5). These results show that UvbZIP6 negatively regulated the responses to hyperosmotic, oxidative, and SDS stresses but positively regulated the CR and CFW stress responses, indicating that UvbZIP6 is involved in stress responses of *U. virens*.

### UvbZIP6 contributes to false smut ball formation but not the infection

The inoculation experiments were performed to determine the role of UvbZIP6 in the pathogenicity of *U. virens*. Although no smut balls were observed in the rice spikelets inoculated with the Δ*UvbZIP6* mutants at 21 dpi (Fig. 6a, b), the mutants could successfully infect rice plants, and no significant difference was observed in the number of infected spikelets caused by the WT, Δ*UvbZIP6*, and complemented strains (Fig. 6c). Further observation found that abundant mycelia were observed in the spikelets infected with the WT and Δ*UvbZIP6* mutants at 11 dpi; at 15 dpi, the smut balls began to form in the WT-infected rather than in Δ*UvbZIP6*-infected spikelets; at 18 dpi, WT produced typical mature smut balls. However, no smut balls were observed in plants infected with Δ*UvbZIP6* (Fig. 6d). In addition, the ovarian development of the infected rice plants was investigated. The ovaries infected by Δ*UvbZIP6* remained

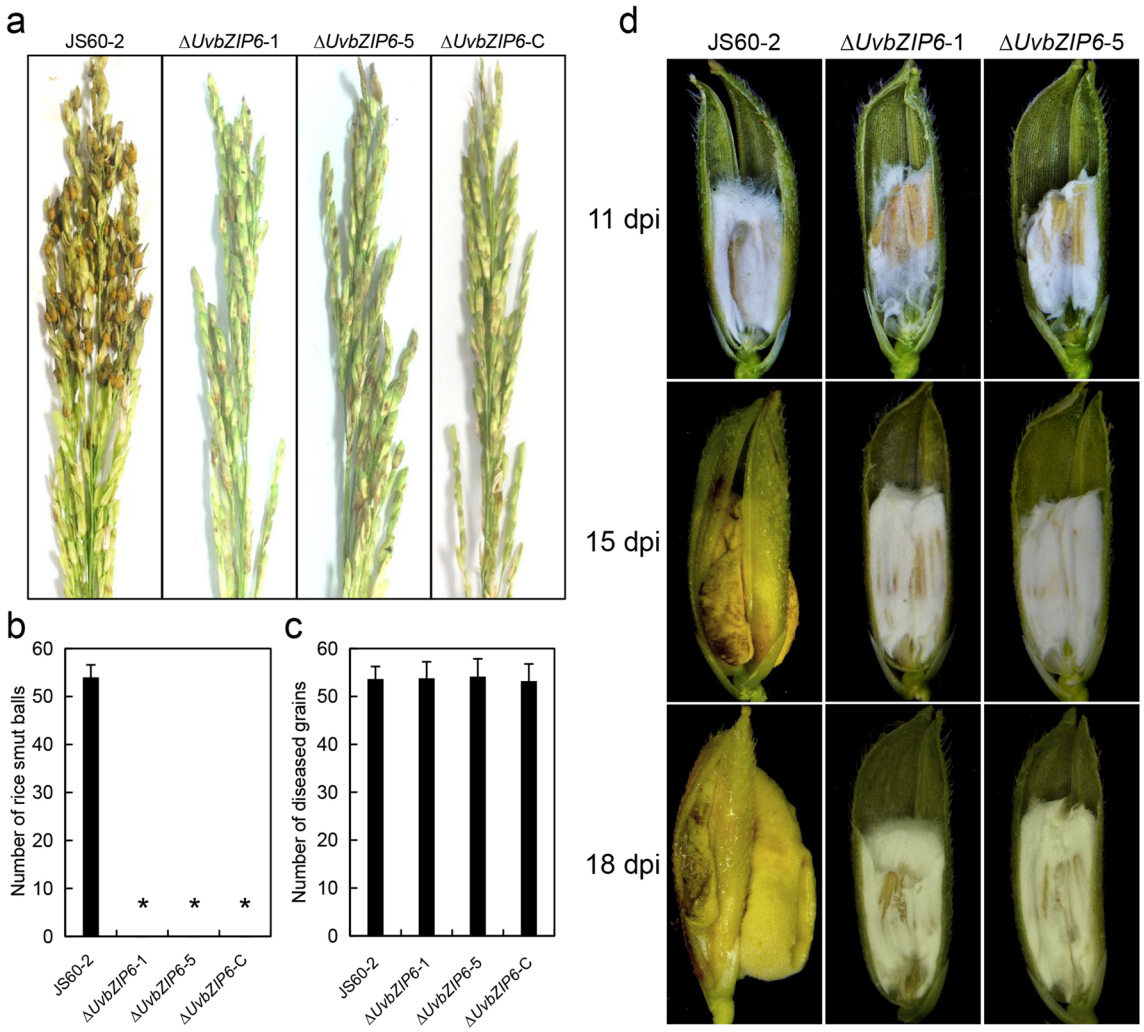


**Fig. 6** UvbZIP6 contributes to false smut formation. **a** Symptoms of rice panicle inoculated with the WT, *UvbZIP6*-knockout mutants, or complemented strains. The suspension containing conidia and mycelia was injected into individual rice panicles, and the symptoms were investigated at 21 dpi. **b** The number of smut balls per panicle produced by the indicted *U. virens* strains. **c** The number of infected grains per rice panicle. **d** Comparison of the infection process of the WT and *UvbZIP6* mutants on rice panicle at 11, 15, and 18 dpi

green (Additional file 1: Figure S6). These results indicate that UvbZIP6 plays an essential role in false smut ball formation.

### Deletion of *UvbZIP6* does not affect the expression of genes associated with grain filling in rice

The *U. virens* infection can induce the expression of grain filling-associated genes by simulating ovary fertilization (Song et al. 2016; Fan et al. 2020). Seven grain filling-associated genes were selected in this study for the transcriptional evaluation to confirm whether these genes were induced. The results showed that these genes were induced in WT- or Δ*UvbZIP6*-inoculated rice plants, although their expression levels varied at different stages of infection (Fig. 7). Generally, the expression profiles of these genes after inoculation with WT or Δ*UvbZIP6* were similar, suggesting that the mutants could still manipulate rice to acquire nutrition. These results reveal that the Δ*UvbZIP6* mutants could not form false smut likely due to a developmental defect rather than incompetence in nutrient absorption.

### Global transcriptional analysis of the *UvbZIP6* deletion mutants

TFs are important regulators of gene expression. To explore the potential genes regulated by UvbZIP6 in *U. virens*, we used three biological replicates of the WT- or Δ*UvbZIP6*-inoculated rice spikelets for RNA sequence (RNA-seq) analysis at 11 dpi, a crucial early stage for smut ball formation. More than 46 million unique identifier reads were generated per sample (Additional file 2: Table S2); more than 95% of reads were mapped on the *U. virens* or rice genome, most of which were mapped on the *U. virens* genome (Additional file 2: Table S2). A total of 565 differentially expressed genes (DEGs) were detected between the Δ*UvbZIP6* mutant and WT, including 207 up-regulated and 358 down-regulated genes, using a threshold of > twofold change in expression and a *P*-value < 0.05 (Fig. 8a, d; Additional file 2: Table S3). These DEGs were classified using gene ontology (GO) analysis, and were mainly associated with the extracellular region, an integral component of the plasma membrane, vacuolar membrane, and cell periphery within the cellular component category. The DEGs were mainly associated with the molecular functions of oxidoreductase activity, iron ion binding, NADP binding, and methyltransferase activity. Further, among biological processes, they were mainly associated with the glutamine metabolic process, transmembrane transport, and methylation (Fig. 8b, c). Functional enrichment based on KEGG pathways for DEGs in *U. virens* showed that they were associated with metabolic pathways. Determination

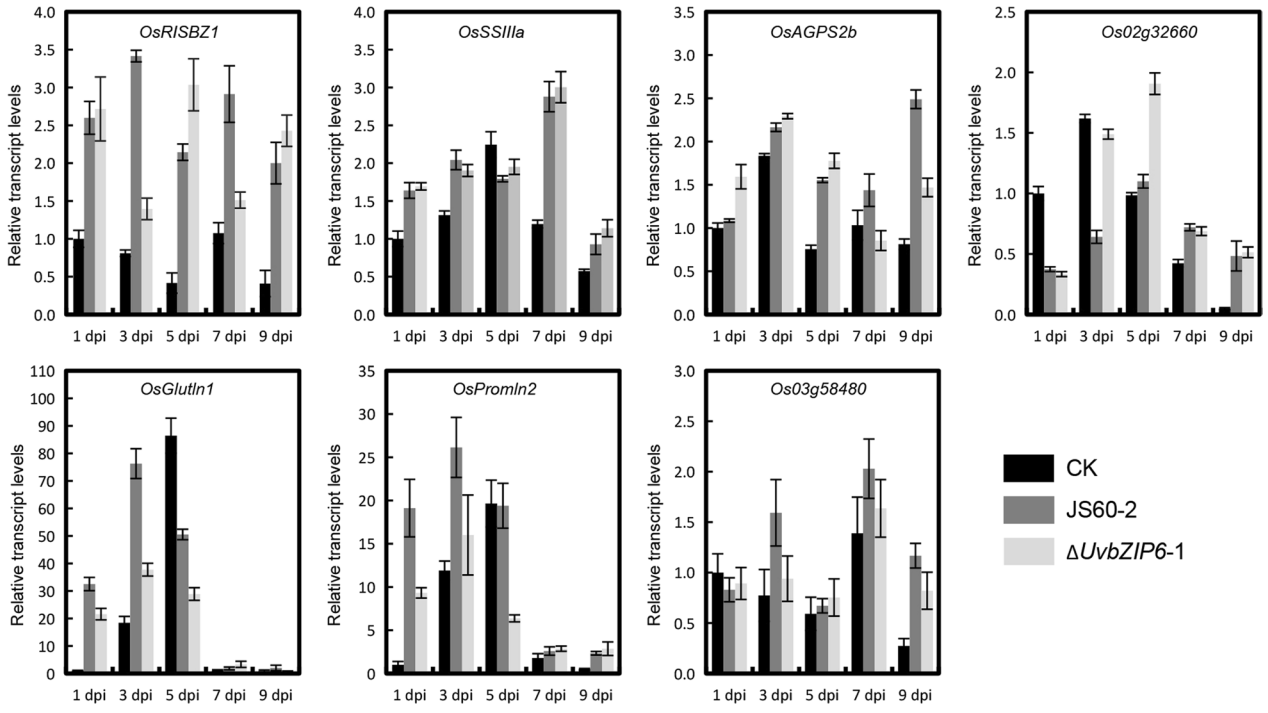


**Fig. 7** Expression profiles of 7 rice filling-related genes after inoculation with the WT or *UvbZIP6*-knockout mutant. The expression levels of the genes were detected at 1, 3, 5, 7, and 9 dpi. Rice plants inoculated with sterile $ddH_2O$ were used as control (CK). The *GAPDH* gene was used as the internal reference. The expression level for CK at 1 dpi was normalized to 1.0

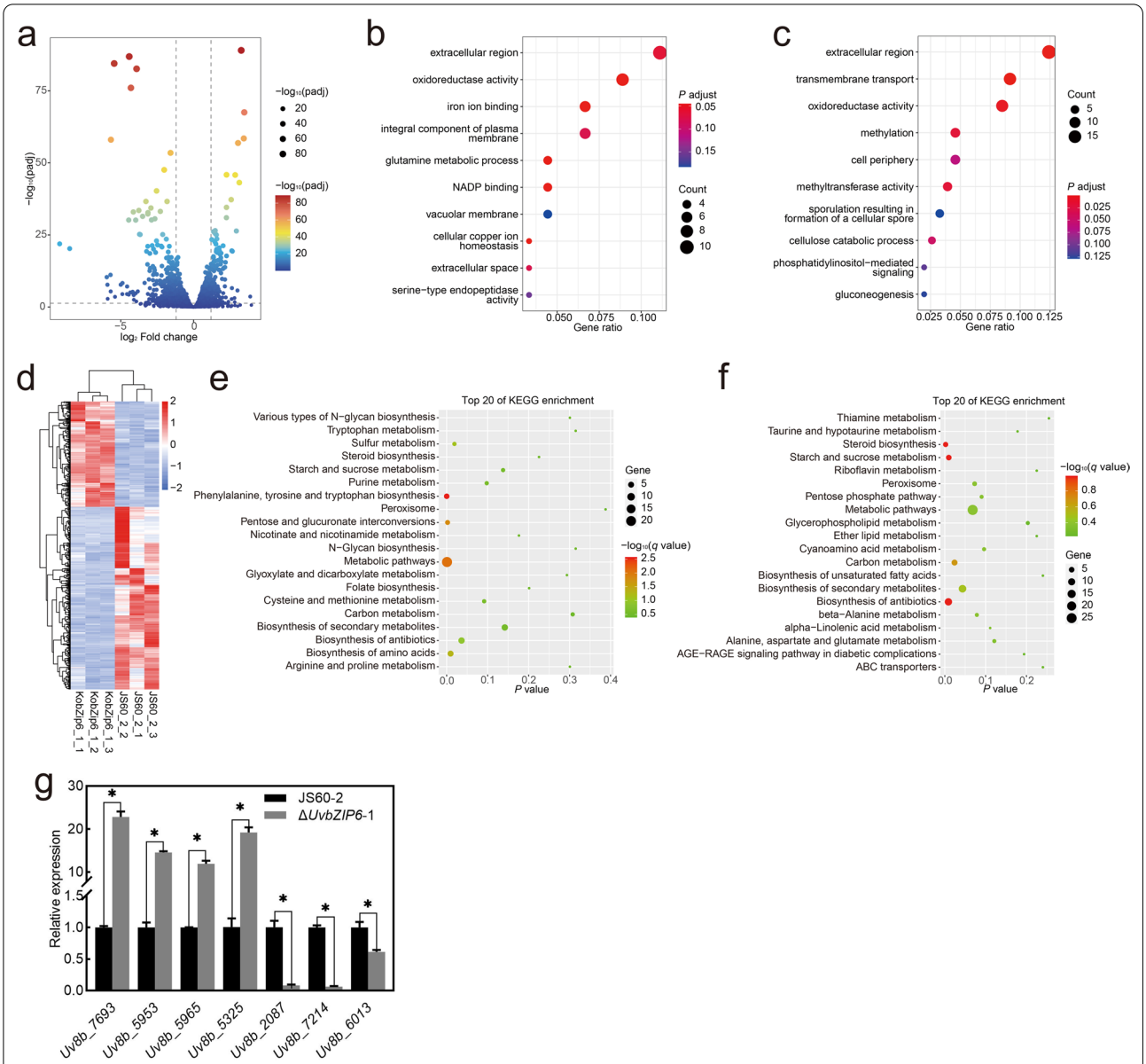


**Fig. 8** Transcriptomic analysis to identify differentially expressed genes (DEGs) between the *UvbZIP6*-knockout mutant and the wild-type strain JS60-2. **a** Volcano plot of DEGs. **b**, **c** Gene ontology enrichment analysis of the DEGs, showing up-regulated DEGs in **b** and down-regulated DEGs in **c**. **d** Heatmap of FPKM-normalized transcript levels of the 565 DEGs in each pair-wise comparison. **e**, **f** Top 20 up-regulated (**e**) and down-regulated DEGs (**f**) in the KEGG enrichment analysis. **g** qPCR analysis to validate the DEGs. The relative transcript level of each gene from Δ*UvbZIP6* was normalized by comparison with the gene from JS60-2 (relative transcript level = 1.0). Asterisks indicate the significant differences between the mutant and JS60-2 ($P < 0.05$). Error bars represent standard deviations

of the top 20 enriched KEGG pathways showed that metabolic pathways, biosynthesis of secondary metabolites, and biosynthesis of antibiotics were the top three enriched pathways (Fig. 8e, f). Seven genes were selected to confirm the gene expression patterns revealed by RNA-seq using qPCR analysis. The expression pattern of each up-regulated or down-regulated gene was consistent with the RNA-seq data (Fig. 8g). These results indicate that *UvbZIP6* may play critical roles in metabolic pathways and biosynthesis of secondary metabolites and antibiotics.

## Discussion

The bZIP proteins are transcription factors that are widely distributed in eukaryotes, some of which are involved in vegetative growth, development, stress

response, and hormonal regulation. However, the orthologs of UvbZIP6 were only found in a few species, indicating its potential specific function. In this study, we found that UvbZIP6 played critical roles in vegetative growth, conidiation, stress response, and false smut formation of *U. virens*.

Some bZIP gene knockout mutants of *M. oryzae* display an increase or decrease in mycelial growth rate, indicating that they are regulators of vegetative growth (Tang et al. 2015). Deletion of *UvbZIP6* in *U. virens* leads to increased vegetative hyphal growth and biomass, which was also observed in *UvBI-1* knockout mutants (Xie et al. 2019). In *Phytophthora sojae*, silencing *PsBZP32* leads to decreased cyst germination, but does not affect mycelial growth, sporangium formation, and oospore production (Sheng et al. 2021). In *M. oryzae*, disrupting the bZIP gene *MoAP1* results in abnormal conidial morphology and reduced conidiation (Guo et al. 2011). The defects in hyphal growth and conidium formation were also observed in *FpAda1*-knockout mutants of *Fusarium pseudograminearum* (Chen et al. 2020). In this study, conidial production was decreased in *UvbZIP6*-knockout mutants, indicating that *UvbZIP6* regulates conidiation in *U. virens*.

A considerable number of bZIPs are involved in stress responses in fungi and oomycetes. In *Peronophythora litchi*, *PlBZP32*-silenced mutants are more sensitive to oxidative stress than the WT strain (Kong et al. 2020). In the plant endophytic fungus *Pestalotiopsis fici*, the deletion of *PfzipA* confers the resistance to oxidative reagents tert-butylhydroperoxide, diamide, and menadione sodium bisulfite (MSB) and increases the sensitivity to $H_2O_2$ (Wang et al. 2015). The bZIP proteins in plants are also involved in stress responses. *ZmbZIP4* is induced under abiotic stress, and overexpression of *ZmbZIP4* leads to increased abscisic acid synthesis and resistance against abiotic stress in maize (Ma et al. 2018). In this study, deletion of *UvbZIP6* resulted in increased resistance against hyperosmotic, oxidative, and SDS stresses; however, the sensitivity to CR and CFW stresses was increased. The CR and CFW are cell wall stresses, and SDS is the stress of membrane stability. These results indicate the different regulatory mechanisms of UvbZIP6 in response to different stresses.

Seven to nine days after inoculation with *U. virens* has been demonstrated to be a crucial period for the initial formation of false smuts (Song et al. 2016). In our study, *UvbZIP6* showed the highest expression level at 7 dpi. At this time, host colonization by *U. virens* has been accomplished, and abundant mycelia are produced, suggesting the potential role of *UvbZIP6* in regulating hyphal transition. Overexpressing *DKM*, a bZIP gene in *Arabidopsis*, causes defects in vegetative and reproductive development, whereas *DKM* deletion mutants have more floral buds and longer fruits (Lozano-Sotomayor et al. 2016). In addition to reducing vegetative growth, asexual sporulation, and virulence, the deletion of *Fpo1* in *F. graminearum* increases the production and maturation of perithecia (Shin et al. 2020). In this study, although *UvbZIP6*-knockout mutants caused a successful infection, they lost the ability to form false smut balls, indicating that UvbZIP6 plays a critical role in the formation of false smut balls.

In this study, we found that the complemented strains could not form false smut balls, but other phenotypes were similar to those of the WT strain. The phenomenon that complemented strains cannot restore full virulence of the WT has also been shown in a previous study (Zhang et al. 2020). This indicates that not all genes can be completely complemented in *U. virens*.

The bZIP domain contains a basic DNA binding region and an adjacent leucine zipper that enables bZIP dimerization (Dröge-Laser et al. 2018). TubZIP28 increases starch synthesis in wheat by binding the promoter and upregulating the cytosolic AGPase-coding gene (Song et al. 2020). By regulating the expression of *VdNut1*, VdAtf1 affected penetration peg formation and nutritional deficiency tolerance (Tang et al. 2020). Here, RNA-seq data revealed the DEGs involved in metabolic pathways, biosynthesis of secondary metabolites, and biosynthesis of antibiotics. These results imply that UvbZIP6 contributes to false smut formation by participating in the regulation of metabolic pathways. Therefore, further studies should be conducted to elucidate the regulatory mechanism of this bZIP protein.

## Conclusions

In this study, we found that *UvbZIP6* is a negative regulator of vegetative growth and stress tolerance in *U. virens*. Furthermore, deletion of *UvbZIP6* abolishes the ability of *U. virens* to generate false smut balls, indicating its critical role in this biological process. However, although numerous DEGs were identified in *UvbZIP6*-knockout mutants, the genes directly regulated by *UvbZIP6* are still unknown. Therefore, genes regulated by UvbZIP6 should be identified in future studies to reveal the molecular mechanism underlying false smut formation in *U. virens*.

## Methods

### Sequence analysis

The data of the gene and protein used in this study were downloaded from the *U. virens* database (https://www.ncbi.nlm.nih.gov/nuccore/JHTR00000000). Sequence alignments were performed using BioEdit, and phylogenetic analyses were performed using MEGA 7.0 based on a neighbor-joining algorithm (Kumar et al. 2016).

### Fungal strains and cultural media

The *U. virens* WT strain JS60-2 and *UvbZIP6*-knockout mutants were cultured on potato sucrose agar (PSA) medium at 27 °C. The strains were cultured on PSA (potato 200 g/L, sucrose 20 g/L, and agar 15 g/L), potato dextrose agar (PDA) (potato 200 g/L, D-glucose 20 g/L, and agar 15 g/L), and yeast tryptone glucose (YTD) (yeast extract, 1 g/L, tryptone 1 g/L, D (+) -glucose 10 g/L, and agar 15 g/L) medium for assessment of colony growth rate. For biomass assay, six plugs (3 mm in diameter) of a fungal strain were cultured in 50 mL of PSB (PSA without agar) medium at 160 rpm and 27 °C for 7 days; mycelia were collected by filtration through two layers of cotton gauze, and the weights were measured after drying at 50 °C for 3 days. The strains were incubated in PSB medium at 160 rpm and 27 °C for 7 days for conidiation. Then, the cultured mixtures were filtrated, and conidia concentrations were measured using a hemocytometer. For the germination test, the conidia were spread on the plates; three regions were selected on one plate, and 100 conidia were observed within each region. To test the stress tolerance, we evaluated *U. virens* strains after 14 days of growth on PSA medium containing 0.5 M NaCl, 0.9 M sorbitol, 0.03% $H_2O_2$, 0.04% SDS, 120 μg/mL CFW or 200 μg/mL CR. The inhibition rate was calculated as follows: Inhibition rate (%) = [(the average colony diameter on PSA − the average colony diameter on PSA with a stress agent) / the average colony diameter on PSA] × 100. All the experiments were repeated three times with three replicates each time.

### Gene expression analysis

Total RNA samples were isolated using TRIzol reagent (Invitrogen), and the cDNA was synthesized using a Thermo scientific RevertAid First Stand cDNA Synthesis Kit (Thermo Fisher Scientific). The reaction mixtures were diluted six times and used as templates. qPCR was performed using a CFX96 Real-Time PCR Detection System (Bio-Rad Laboratories Inc.). The relative expression level of the gene was calculated using the $2^{-\Delta\Delta Ct}$ method. Data from three biological replicates were used to calculate the mean and standard deviation. The RT-PCR was conducted with 30 cycles to confirm the deletion and reintroduction of the *UvbZIP6* gene with the indicating primers. All primers used in this assay are listed in Additional file 2: Table S1.

### Construction and complementation of the *UvbZIP6* deletion mutant

For the CRISPR/Cas system vector construction, a short cassette was generated by annealing the sense (CRISPR_UvbZIP6-F) and antisense (CRISPR_UvbZIP6-R) oligonucleotides (Additional file 2: Table S1) and inserted between the two *Esp*3I sites of pCas9: tRp-gRNA vector as previously described (Liang et al. 2018). The *UvbZIP6* gene replacement construct was generated by the double-joint PCR method (Yu et al. 2004). Briefly, fragments of a 1.8-kb upstream flanking sequence and a 1.9-kb downstream flanking sequence of *UvbZIP6* were amplified from *U. virens* genomic DNA using the primers of first-round of amplification. Next, the 5′ and 3′ partials of *hph* were amplified using the primers HYG-F and H3, and H2 and HYG-R, respectively. The upstream and downstream flanking sequences were joined with the 5′ and 3′ partials of the *hph* gene, respectively. The CRISPR vector and recombinant fragments were introduced into protoplasts using protoplast-mediated transformation. To generate the complemented strains of the *UvbZIP6* deletion mutants, the full-length genomic sequence with a 2.0 kb upstream and 0.5 kb downstream flanking sequence of the gene was amplified and inserted into the pKNRG823 vector that contains a geneticin resistance gene. Then, the vector was transformed into the mutant using protoplast-mediated transformation.

### Pathogenicity and plant infection assays

The *U. virens* strains were inoculated in the susceptible rice cultivar (Wanxian-98) following the previous descriptions (Jia et al. 2015; Song et al. 2016). Mycelial plugs cut from 14-day-old fungal colony were placed into PSB medium and shaken at 160 rpm and 27 °C for 7 days; Mycelia were collected and crushed, and the conidia were measured and adjusted to a concentration of $5 \times 10^6$/mL with PSB. Approximately 2 mL of the suspension containing conidia and mycelia was injected into a single rice panicle at the late booting stage (3–5 days before heading). Inoculated plants were maintained in a greenhouse at 27 °C with 90–100% relative humidity (RH) for 7 days, and then they were placed at 27 °C and 80% RH until the symptoms appeared. The number of smut balls was measured 21 days after inoculation. At least three independent biological experiments were performed with at least 12 replicates in each test.

### RNA sequencing

RNA extraction, library preparation, and data analysis of high throughput sequencing were conducted by Kangce Technology Co., LTD (Wuhan, China). Total RNAs was extracted using TRIzol reagent (Invitrogen). A total of 2 μg total RNA was used for stranded RNA sequencing library preparation using KC-DigitalTM Stranded mRNA Library Prep Kit for Illumina® (Catalog NO. DR08502, Seqhealth Technology Co., Ltd. Wuhan, China). The 200–500 bp products were enriched, quantified, and finally sequenced on Illumina Novaseq 6000. Raw sequencing data were first filtered by Trimmomatic (version

0.36), and clean reads were further treated with in-house scripts to eliminate duplication bias introduced during library preparation and sequencing. They were mapped to the reference genome of *Oryza sativa* Japonica group (https://www.ncbi.nlm.nih.gov/genome/10) and *U. virens* (http://www.ncbi.nlm.nih.gov/nuccore/JHTR00000000.1) using STAR software (version 2.5.3a) with default parameters. Reads mapped to the exon regions of each gene were counted by featureCounts (Subread-1.5.1; Bioconductor), and then reads per kilobase million (RPKM) were calculated. Genes differentially expressed between groups were identified using the edgeR package (version 3.12.1). The false discovery rate (FDR) corrected *p*-value cut-off of 0.05 and fold-change cut-off of two was used to judge the statistical significance of gene expression differences. Gene ontology (GO) and Kyoto Encyclopedia of Genes and Genomes (KEGG) enrichment analysis for DEGs were both implemented by KOBAS software (version: 2.1.1) with a corrected *p*-value cut-off of 0.05 to determine statistically significant enrichment. Alternative splicing events were detected using rMATS (version 3.2.5) with an FDR value cut-off of 0.05 and an absolute $\Delta\psi$ value of 0.05.

### Statistical analysis

Statistical analysis of the data was performed using Microsoft Office 2016. The figures were prepared using Microsoft Office 2016 and GraphPad Prism 8.0. Significant difference ($P=0.05$) was determined based on a one-way analysis of variance (ANOVA) and LSD test performed using SPSS Statistics 21.0.

#### Abbreviations

bZIP: Basic leucine zipper; CFW: Calcofluor white; CR: Congo red; dpi: Days post-inoculation; DEGs: Differentially expressed genes; ER: Endoplasmic reticulum; GO: Gene ontology; MSB: Menadione sodium bisulfite; NO: Nitric oxide; ORF: Open reading frame; RH: Relative humidity; RNA-seq: RNA sequence; ROS: Reactive oxygen species; SDS: Sodium dodecyl sulfate; TFs: Transcription factors; WT: Wild type.

## Supplementary Information

The online version contains supplementary material available at https://doi.org/10.1186/s42483-022-00137-x.

**Additional file 1: Figure S1.** Sequence alignment of UvbZIP6 proteins from *U. virens* JS60-2 and UV-8b strains. **Figure S2.** Target knockout of *UvbZIP6* and transformants verification. **a** PCR verification of knockout transformants using different primer pairs. The DNA samples were collected from mycelia cultured in PSB medium for 7 days. The fragments of *β-tubulin* were amplified as a control to test DNA quality. WT indicates the wild-type strain JS60-2. **b** Schematic of the strategy for target knockout of *UvbZIP6*. The arrows show the primers in this study. **Figure S3.** Verification of the *UvbZIP6* complemented strains. **a** The complemented transformants were amplified using different primer pairs. The plasmid, Δ*UvbZIP6*-5, and WT indicate the complemented vector containing *UvbZIP6* fragment, *UvbZIP6*-knockout mutant, and wild-type JS60-2 strain, respectively. **b** The complementation strategy and primers used in the verification. **Figure S4.** Detection of *UvbZIP6* expression in *UvbZIP6*-knockout mutants and complemented strains by semiquantitative RT-PCR. The RNA samples were collected from mycelia cultured in PSB medium for 7 days. The fragments of *β-tubulin* were amplified as reference. **Figure S5.** Conidia germination rate of the tested strains. The conidia were spread on water agar (WA) or PSA plates. **Figure S6.** Microscopic observation of rice ovary after inoculation with JS60-2 or *UvbZIP6*-knockout mutants.

**Additional file 2: Table S1.** The primers used in this study. **Table S2.** Quality evaluation and statistical analysis of sample sequencing data. **Table S3.** List of up- or down-regulated genes in the *UvbZIP6*-knockout mutant.

#### Acknowledgements

We thank Prof. JinRong Xu (Northwest A&F University, Purdue University) for providing the CRISPR-Cas9 system plasmid.

#### Authors' contributions

JQ, YW, WY, and CL designed experiments; JQ, YW, MC, YL, LG, YD, CX, and RW performed the experiments; YW, MC, PZ, YL, WY, and CL analyzed the data; JQ, YW, WY, and CL wrote the manuscript. All authors read and approved the final manuscript.

#### Funding

This work was supported by the Key Research & Development Program of Hubei Province (Grant No. 2021BBA236), the National Natural Science Foundation of China (Grant No. 31701736), and National Key Research and Development Program (Grant No. 2016YFD0300700).

#### Availability of data and materials

Not applicable.

## Declarations

#### Ethics approval and consent to participate

Not applicable.

#### Consent for publication

Not applicable.

#### Competing interests

The authors declare that they have no competing interests.

Received: 5 November 2021 Accepted: 15 August 2022
Published online: 29 August 2022

#### References

Amich J, Schafferer L, Haas H, Krappmann S. Regulation of sulphur assimilation is essential for virulence and affects iron homeostasis of the human-pathogenic mould *Aspergillus fumigatus*. PLoS Pathog. 2013;9: e1003573. https://doi.org/10.1371/journal.ppat.1003573.

An JP, Qu FJ, Yao JF, Wang XN, You CX, Wang XF, et al. The bZIP transcription factor MdHY5 regulates anthocyanin accumulation and nitrate assimilation in apple. Hortic Res. 2017;4:17023. https://doi.org/10.1038/hortres.2017.23.

Chen L, Ma Y, Zhao J, Geng X, Chen W, Ding S, et al. The bZIP transcription factor FpAda1 is essential for fungal growth and conidiation in *Fusarium pseudograminearum*. Curr Genet. 2020;66:507–15. https://doi.org/10.1007/s00294-019-01042-1.

Dröge-Laser W, Weiste C. The C/S1 bZIP network: a regulatory hub orchestrating plant energy homeostasis. Trends Plant Sci. 2018;23:422–33. https://doi.org/10.1016/j.tplants.2018.02.003.

Dröge-Laser W, Snoek BL, Snel B, Weiste C. The *Arabidopsis* bZIP transcription factor family—an update. Curr Opin Plant Biol. 2018;45:36–49. https://doi.org/10.1016/j.pbi.2018.05.001.

Fan J, Liu J, Gong ZY, Xu PZ, Hu XH, Wu JL, et al. The false smut pathogen *Ustilaginoidea virens* requires rice stamens for false smut ball formation.

Environ Microbiol. 2020;22:646–59. https://doi.org/10.1111/1462-2920.14881.
Fernández-Vázquez J, Vargas-Pérez I, Sansó M, Buhne K, Carmona M, Paulo E, et al. Modification of tRNA(Lys) UUU by elongator is essential for efficient translation of stress mRNAs. PLoS Genet. 2013;9: e1003647. https://doi.org/10.1371/journal.pgen.1003647.
Guo M, Chen Y, Du Y, Dong Y, Guo W, Zhai S, et al. The bZIP transcription factor MoAP1 mediates the oxidative stress response and is critical for pathogenicity of the rice blast fungus *Magnaporthe oryzae*. PLoS Pathog. 2011;7: e1001302. https://doi.org/10.1371/journal.ppat.1001302.
Hao X, Zhong Y, Nützmann HW, Fu X, Yan T, Shen Q, et al. Light-induced artemisinin biosynthesis is regulated by the bZIP transcription factor AaHY5 in *Artemisia annua*. Plant Cell Physiol. 2019;60:1747–60. https://doi.org/10.1093/pcp/pcz084.
Hu Z, Dang Y, Liu C, Zhou L, Liu H. Acute exposure to ustiloxin A affects growth and development of early life zebrafish, *Danio Rerio*. Chemosphere. 2019;226:851–7. https://doi.org/10.1016/j.chemosphere.2019.04.002.
Jia Q, Lv B, Guo MY, Luo CX, Zheng L, Hsiang T, et al. Effect of rice growth stage, temperature, relative humidity and wetness duration on infection of rice panicles by *Villosiclava virens*. Eur J Plant Pathol. 2015;141:15–25. https://doi.org/10.1007/s10658-014-0516-4.
Kong S, Park SY, Lee YH. Systematic characterization of the bZIP transcription factor gene family in the rice blast fungus, *Magnaporthe Oryzae*. Environ Microbiol. 2015;17:1425–43. https://doi.org/10.1111/1462-2920.12633.
Kong G, Chen Y, Deng Y, Feng D, Jiang L, Wan L, et al. The basic leucine zipper transcription factor PlBZP32 associated with the oxidative stress response is critical for pathogenicity of the lychee downy blight oomycete *Peronophythora litchii*. mSphere. 2020;5:e00261-20. https://doi.org/10.1128/mSphere.00261-20.
Kumar S, Stecher G, Tamura K. MEGA7: molecular evolutionary genetics analysis version 7.0 for bigger datasets. Mol Biol Evol. 2016;33:1870–4. https://doi.org/10.1093/molbev/msw054.
Lambert SA, Jolma A, Campitelli LF, Das PK, Yin Y, Albu M, et al. The human transcription factors. Cell. 2018;172:650–65. https://doi.org/10.1016/j.cell.2018.01.029.
Liang YF, Han Y, Wang CF, Jiang C, Xu JR. Targeted deletion of the *USTA* and *UvSLT2* genes efficiently in *Ustilaginoidea virens* with the CRISPR-Cas9 system. Front Plant Sci. 2018;9:699. https://doi.org/10.3389/fpls.2018.00699.
Liu C, Ou S, Mao B, Tang J, Wang W, Wang H, et al. Early selection of *bZIP73* facilitated adaptation of *japonica* rice to cold climates. Nat Commun. 2018;9:3302. https://doi.org/10.1038/s41467-018-05753-w.
Liu XH, Lyu YS, Yang W, Yang ZT, Lu SJ, Liu JX. A membrane-associated NAC transcription factor OsNTL3 is involved in thermotolerance in rice. Plant Biotechnol J. 2020;18:1317–29. https://doi.org/10.1111/pbi.13297.
López-Berges MS, Capilla J, Turrà D, Schafferer L, Matthijs S, Jöchl C, et al. HapX-mediated iron homeostasis is essential for rhizosphere competence and virulence of the soilborne pathogen *Fusarium oxysporum*. Plant Cell. 2012;24:3805–22. https://doi.org/10.1105/tpc.112.098624.
Lozano-Sotomayor P, Chávez Montes RA, Silvestre-Vañó M, Herrera-Ubaldo H, Greco R, Pablo-Villa J, et al. Altered expression of the bZIP transcription factor DRINK ME affects growth and reproductive development in *Arabidopsis thaliana*. Plant J. 2016;88:437–51. https://doi.org/10.1111/tpj.13264.
Lu SJ, Yang ZT, Sun L, Sun L, Song ZT, Liu JX. Conservation of IRE1-regulated bZIP74 mRNA unconventional splicing in rice (*Oryza sativa* L.) involved in ER stress responses. Mol Plant. 2012;5:504–14. https://doi.org/10.1093/mp/ssr115.
Lv B, Zheng L, Liu H, Tang JT, Hsiang T, Huang JB. Use of random T-DNA mutagenesis in identification of gene *UvPRO1*, a regulator of conidiation, stress response, and virulence in *Ustilaginoidea virens*. Front Microbiol. 2016;7:2086. https://doi.org/10.3389/fmicb.2016.02086.
Ma H, Liu C, Li Z, Ran Q, Xie G, Wang B, et al. ZmbZIP4 contributes to stress resistance in maize by regulating ABA synthesis and root development. Plant Physiol. 2018;178:753. https://doi.org/10.1104/pp.18.00436.
Sheng Y, Lin L, Chen H, Pu T, Liu X, Dong S, et al. The bZIP transcription factor PsBZP32 is involved in cyst germination, oxidative stress response, and pathogenicity of *Phytophthora sojae*. Phytopathol Res. 2021;3:1. https://doi.org/10.1186/s42483-020-00078-3.
Shin J, Bui D-C, Kim S, Jung SY, Nam HJ, Lim JY, et al. The novel bZIP transcription factor Fpo1 negatively regulates perithecial development by modulating carbon metabolism in the ascomycete fungus *Fusarium graminearum*. Environ Microbiol. 2020;22:2596–612. https://doi.org/10.1111/1462-2920.14960.
Song JH, Wei W, Lv B, Lin Y, Yin WX, Peng YL, et al. Rice false smut fungus hijacks the rice nutrients supply by blocking and mimicking the fertilization of rice ovary. Environ Microbiol. 2016;18:3840–9. https://doi.org/10.1111/1462-2920.13343.
Song Z, Yin Y, Lin Y, Du F, Ren G, Wang Z. The bZIP transcriptional factor activator protein-1 regulates *Metarhizium rileyi* morphology and mediates microsclerotia formation. Appl Microbiol Biotechnol. 2018;102:4577–88. https://doi.org/10.1007/s00253-018-8941-5.
Song Y, Luo G, Shen L, Yu K, Yang W, Li X, et al. TubZIP28, a novel bZIP family transcription factor from *Triticum urartu*, and TabZIP28, its homologue from *Triticum aestivum*, enhance starch synthesis in wheat. New Phytol. 2020;226:1384–98. https://doi.org/10.1111/nph.16435.
Tang W, Ru Y, Hong L, Zhu Q, Zuo R, Guo X, et al. System-wide characterization of bZIP transcription factor proteins involved in infection-related morphogenesis of *Magnaporthe oryzae*. Environ Microbiol. 2015;17:1377–96. https://doi.org/10.1111/1462-2920.12618.
Tang C, Li T, Klosterman SJ, Tian C, Wang Y. The bZIP transcription factor VdAtf1 regulates virulence by mediating nitrogen metabolism in *Verticillium dahliae*. New Phytol. 2020;226:1461–79. https://doi.org/10.1111/nph.16481.
Wang X, Wu F, Liu L, Liu X, Che Y, Keller NP, et al. The bZIP transcription factor PfZipA regulates secondary metabolism and oxidative stress response in the plant endophytic fungus *Pestalotiopsis fici*. Fungal Genet Biol. 2015;81:221–8. https://doi.org/10.1016/j.fgb.2015.03.010.
Xie SL, Wang YF, Wei W, Li CY, Liu Y, Qu JS, et al. The Bax inhibitor UvBI-1, a negative regulator of mycelial growth and conidiation, mediates stress response and is critical for pathogenicity of the rice false smut fungus *Ustilaginoidea virens*. Curr Genet. 2019;65:1185–97. https://doi.org/10.1007/s00294-019-00970-2.
Yin WB, Amaike S, Wohlbach DJ, Gasch AP, Chiang YM, Wang CCC, et al. An *Aspergillus nidulans* bZIP response pathway hardwired for defensive secondary metabolism operates through *aflR*. Mol Microbiol. 2012;83:1024–34. https://doi.org/10.1111/j.1365-2958.2012.07986.x.
Yin WX, Cui P, Wei W, Lin Y, Luo CX. Genome-wide identification and analysis of the basic leucine zipper (bZIP) transcription factor gene family in *Ustilaginoidea virens*. Genome. 2017;60:1059–67. https://doi.org/10.1139/gen-2017-0089.
Yu JH, Hamari Z, Han KH, Seo JA, Reyes-Dominguez Y, Scazzocchio C. Double-joint PCR: a PCR-based molecular tool for gene manipulations in filamentous fungi. Fungal Genet Biol. 2004;41:973–81. https://doi.org/10.1016/j.fgb.2004.08.001.
Yu J, Yu M, Song T, Cao H, Pan X, Yong M, et al. A homeobox transcription factor UvHOX2 regulates chlamydospore formation, conidiogenesis, and pathogenicity in *Ustilaginoidea virens*. Front Microbiol. 2019;10:1071. https://doi.org/10.3389/fmicb.2019.01071.
Zhang Y, Zhang K, Fang A, Han Y, Yang J, Xue M, et al. Specific adaptation of *Ustilaginoidea virens* in occupying host florets revealed by comparative and functional genomics. Nat Commun. 2014;5:3849. https://doi.org/10.1038/ncomms4849.
Zhang CY, Liu J, Zhao T, Gomez A, Li C, Yu CS, et al. A drought-inducible bZIP transcription factor OsABF1 delays reproductive timing in rice. Plant Physiol. 2016;171:334–43. https://doi.org/10.1104/pp.16.01691.
Zhang C, Li C, Liu J, Lv Y, Yu C, Li H, et al. The OsABF1 transcription factor improves drought tolerance by activating the transcription of *COR413-TM1* in rice. J Exp Bot. 2017;68:4695–707. https://doi.org/10.1093/jxb/erx260.
Zhang N, Yang JY, Fang AF, Wang JY, Li DY, Li YJ, et al. The essential effector SCRE1 in *Ustilaginoidea virens* suppresses rice immunity via a small peptide region. Mol Plant Pathol. 2020;21:445–59. https://doi.org/10.1111/mpp.12894.